

A UV Complete Framework of Freeze-in Massive Particle Dark Matter

Anirban Biswas,^{1,*} Debasish Borah,^{1,†} and Arnab Dasgupta^{2,‡}

¹*Department of Physics, Indian Institute of Technology Guwahati, Assam 781039, India*

²*School of Liberal Arts, Seoul-Tech, Seoul 139-743, Korea*

Abstract

We propose a way to generate tiny couplings of freeze-in massive particle dark matter with the Standard Model particles dynamically by considering an extension of the electroweak gauge symmetry. The dark matter is considered to be a singlet under this extended gauge symmetry which we have assumed to be the one in a very widely studied scenario called left-right symmetric model. Several heavy particles, that can be thermally inaccessible in the early Universe due to their masses being greater than the reheat temperature after inflation, can play the role of portals between dark matter and Standard Model particles through one loop couplings. Due to the loop suppression, one can generate the required non-thermal dark matter couplings without any need of highly fine tuned Yukawa couplings beyond that of electron Yukawa with the Standard Model like Higgs boson. We show that generic values of Yukawa couplings as large as $\mathcal{O}(0.01)$ to $\mathcal{O}(1)$ can keep the dark matter out of thermal equilibrium in the early Universe and produce the correct relic abundance later through the freeze-in mechanism. Though the radiative couplings of dark matter are tiny as required by the freeze-in scenario, the associated rich particle sector of the model can be probed at ongoing and near future experiments. The allowed values of dark matter mass can remain in a wide range from keV to TeV order keeping the possibilities of warm and cold dark matter equally possible.

*Electronic address: anirban.biswas@iitg.ernet.in

†Electronic address: dborah@iitg.ernet.in

‡Electronic address: arnabdasgupta@protonmail.ch

I. INTRODUCTION

In view of several astrophysical and cosmological evidences, the existence of non-baryonic form of matter, or the so called Dark Matter (DM) in large amount in the present Universe has become an irrefutable fact. Among these evidences, the galaxy cluster observations by Fritz Zwicky [1] back in 1933, observations of galaxy rotation curves in 1970's [2], the more recent observation of the bullet cluster [3] and results from several satellite borne cosmology experiments like WMAP [4] and Planck [5] are the most prominent ones. The precise measurements of the cosmology experiments reveal that more than 80% matter content of our Universe is in the form of this non-baryonic or DM form. The amount of DM present in the Universe is often expressed by a quantity $\Omega_{\text{DM}}h^2$, which is called the relic density of DM and it is the ratio of present mass density of DM by the critical density of the Universe. The value of DM relic density at the present epoch is $0.1172 \leq \Omega_{\text{DM}}h^2 \leq 0.1226$ at 67% C.L. [5]. Here $h = \frac{\mathbf{H}_0}{100 \text{ km s}^{-1} \text{ Mpc}^{-1}}$ is a parameter of order unity while \mathbf{H}_0 being the present value of the Hubble parameter.

In spite these astrophysical and cosmological evidences of DM, the information regarding the constituents and origin of DM still remains unknown to us. One of the well motivated and most studied scenario is to assume the thermal origin of DM [6, 7], where DM particles were produced thermally at the early Universe and depending upon the mass and interaction strength, DM maintained both thermal and chemical equilibrium with the plasma upto a certain temperature of the Universe. Decoupling of DM from the thermal bath particles occurred at around a temperature T_f , which is known as the freeze-out temperature, where the interaction rate of DM dropped below the expansion rate of the Universe governed by the Hubble parameter H . Being decoupled from the rest of the plasma these DM particles becomes thermal relic whose density, after decoupling, is only affected by the expansion of the Universe. The list of criteria a particle DM candidate should fulfil rules out all the Standard Model (SM) particles from being DM candidates, leading to several beyond Standard Model (BSM) proposals in the last few decades. Most of the thermal DM candidates studied in the literature fall into a category called weakly interacting massive particle (WIMP) [8–10], which has mass in the range of few GeV to few TeV and weak scale couplings. The interesting coincidence that a DM particle having mass and couplings around the electroweak scale can give rise to the correct dark matter relic abundance is often referred to as the *WIMP Miracle*.

Now, if such type of particles whose interactions are of the order of electroweak interactions really exist then we should expect their signatures in various DM direct detection experiments where the recoil energies of detector nuclei scattered by DM particles are being measured. However, after decades of running, direct detection experiments are yet to observe any DM-nucleon scattering [11–13]. The absence of dark matter signals from the direct detection experiments have progressively lowered the exclusion curve in its mass-cross section plane. With such high precision measurements, the WIMP-nucleon cross section will soon overlap with the neutrino-nucleon cross section. Similar null results have been also reported by other direct search experiments like the large hadron collider (LHC) giving upper limits on DM interactions with the SM particles. A recent summary of collider searches for DM can be found in [14]. Although such null results could indicate a very constrained region of WIMP parameter space, they have also motivated the particle physics community to look for beyond the thermal WIMP paradigm where the interaction scale of DM particle can be much lower than the scale of weak interaction i.e. DM may be more feebly interacting than the thermal WIMP paradigm.

One of the viable alternatives of WIMP paradigm, which may be a possible reason of null results at various direct detection experiments, is to consider the non-thermal origin of DM [15]. In this scenario, the initial number density of DM in the early Universe is negligible and it is assumed that the interaction strength of DM with other particles in the thermal bath is so feeble that it never reaches thermal equilibrium at any epoch in the early Universe. In this set up, DM is mainly produced from the out of equilibrium decays of some heavy particles in the plasma. It can also be produced from the scatterings of bath particles, however if same couplings are involved in both decay as well as scattering processes then the former has the dominant contribution to DM relic density over the latter one [15–17]. The production mechanism for non-thermal DM is known as freeze-in and the candidates of non-thermal DM produced via freeze-in are often classified into a group called Freeze-in (Feebly interacting) massive particle (FIMP). For a recent review of this DM paradigm, please see [18]. Now, if the mother particle is in thermal equilibrium with the bath then the maximum production of DM occurs when the temperature of the Universe $T \simeq M_0$, the mass of mother particle. Therefore, the non-thermality criterion enforces the couplings to be extremely tiny via the following condition $\left| \frac{\Gamma}{\mathbf{H}} \right|_{T \simeq M_0} < 1$ [19], where Γ is the decay width. For the case of scattering, one has to replace Γ by the interaction rate $n_{\text{eq}} \langle \sigma v \rangle$, n_{eq} being the

equilibrium number density of mother particle. These types of freeze-in scenarios are known as IR-freeze-in [16, 18, 20–26] where DM production is dominated by the lowest possible temperature at which it can occur i.e. $T \sim M_0$, since for $T < M_0$, the number density of mother particle becomes Boltzmann suppressed. Here DM interacts with the visible sector via renormalizable operators (dimension $d \leq 4$) only. There may be a situation in IR-freeze-in, where mother particle itself is out of thermal equilibrium and in such cases, first one has to calculate the distribution function of mother particle considering its all possible production and decay modes. This distribution function is necessary to compute the non-thermal ¹ averages of decay width and annihilation cross sections. Once we know these quantities, the Boltzmann equation for the non-thermal DM can be solved in terms of its comoving number density following the usual procedure [24, 25].

As mentioned earlier that to maintain a situation where DM remains out of thermal equilibrium, one needs extremely tiny couplings of DM with the particles in the plasma. However, theoretically, the origin of such extremely low values of couplings is in general, not obvious. One of the possible explanation of such feeble interactions is to consider DM to be connected to the visible sector via non-renormalizable higher dimensional effective operators. This results in a different type of freeze-in mechanism known as UV-freeze-in [15, 27, 28], where the comoving number density of DM is directly proportional to reheat temperature T_{RH} of the Universe and thus sensitive to the early Universe cosmology. Another interesting way to generate tiny dimensionless couplings is through the recently proposed clockwork mechanism [29, 30] which has been recently explored in the context of freeze-in DM by the authors of [31, 32]. In this work, we try to explain the origin of such tiny couplings by considering a renormalizable gauge extension of the SM where FIMP couplings with the rest of the particles can arise at radiative level, leading to the required suppression naturally. As an illustrative example, we consider a left-right symmetric gauge extension of SM where the FIMP candidate is a gauge singlet. However, at one loop level the gauge bosons can decay into the FIMP, with several particles going inside the loop. The particles in the loop do have sizeable couplings with FIMP, but that does not lead to thermal production of FIMP DM if the corresponding scattering rates always remain smaller than the expansion rate

¹ Here we use the word non-thermal average to distinguish it from the thermal average where the Maxwell-Boltzmann distribution function is used [25].

of the Universe and their decay into FIMP are kinematically forbidden. However, if same couplings are involved in both scattering as well as the one loop decay, keeping scattering rates out of equilibrium typically makes the decay contribution very small. Another way is to consider these mediator particles to be too heavy to be produced at the end of inflation (having mass more than the reheat temperature). We adopt this approach without going into the details of specific inflationary models and find the predictions for the dark sector. Such an exercise can be carried out for simpler gauge extension of SM as well, but we perform it here for left-right symmetric model (LRSM) which has several other motivations.

Rest of the article is organised as follows. In section II, we discuss our model followed by the details of the calculation of one loop vertex factors of dark matter interactions with the neutral gauge bosons in section III. In section IV we discuss the details of dark matter calculations, results and then finally conclude in section V

II. THE MODEL

The LRSM is one of most highly motivated BSM frameworks which in its generic form [33–37], not only explains the origin of parity violation in weak interactions but also explains the origin of tiny neutrino masses naturally. The gauge symmetry group and the field content of the generic LRSM can also be embedded within grand unified theory (GUT) symmetry groups like $SO(10)$ providing a non-supersymmetric route to gauge coupling unification. The right handed fermions of the SM forms doublet under a new $SU(2)_R$ group in LRSM such that the theory remains parity symmetric at high energy. This necessitates the inclusion of the right handed neutrino as a part of the right handed lepton doublet. To be more appropriate, the gauge symmetry of the Standard Model namely, $SU(3)_c \times SU(2)_L \times U(1)_Y$ is upgraded to $SU(3)_c \times SU(2)_L \times SU(2)_R \times U(1)_{B-L}$ such that the right handed fermions transform as doublets under $SU(2)_R$, making the theory left-right symmetric. The model also has an in-built discrete \mathbb{Z}_2 symmetry or D-parity which ensures the equality of couplings in $SU(2)_{L,R}$ sectors. The effective parity violating electroweak physics at low energy arises as a result of spontaneous breaking of the $SU(2)_R \times U(1)_{B-L} \times D$ to $U(1)_Y$ of the SM.

The minimal LRSM however, does not contain a naturally stable DM candidate. One can of course realise a long lived keV right handed neutrino DM in these models. Such a scenario leading to warm dark matter scenarios has been investigated within LRSM in [38–40]. Due

the presence of $SU(2)_R$ gauge interactions, such a right handed neutrino dark matter can be thermally produced in the early Universe, unlike in typical keV right handed neutrino DM models where non-thermal origin is required [41]. On the other hand, to have WIMP DM type realisation, the minimal LRSM can be extended by additional scalar or fermion multiplets in the spirit of minimal DM scenario [42–44]. Such minimal dark matter scenario in LRSM has been studied recently by the authors of [45, 46]. In these models, the dark matter candidate is stabilised either by a $\mathbb{Z}_2 = (-1)^{B-L}$ subgroup of the $U(1)_{B-L}$ gauge symmetry or due to an accidental symmetry at the renormalisable level due to the absence of any renormalisable operator leading to dark matter decay [47]. Some more studies on left-right dark matter also appeared in the recent works [48–52]. The possibility of right handed neutrino dark matter in a different version of LRSM where the right handed lepton doublets do not contain the usual charged leptons, was also studied in the recent works [53–55].

In this work, we intend to have a purely non-thermal DM within LRSM. We therefore consider gauge singlet fermion N as our DM candidate. We introduce an additional \mathbb{Z}_2 symmetry under which this new singlet fermion is odd and hence can be stable if it happens to be the lightest \mathbb{Z}_2 odd particle. One can also consider scalar singlet DM, but scalars usually have quartic couplings with other scalars and it is often difficult to forbid them from symmetry arguments. We also introduce two copies of vector like fermion doublets ψ and a pair of scalar doublets $H_{L,R}$ to the minimal LRSM. These additional fields play the role of generating interactions of the SM sector with the DM particle N at radiative level, as we will see below.

The relevant Yukawa couplings for the Standard Model fermion masses can be written as

$$\begin{aligned} \mathcal{L}_Y^{SM} = & y_{ij} \bar{\ell}_{iL} \Phi \ell_{jR} + y'_{ij} \bar{\ell}_{iL} \tilde{\Phi} \ell_{jR} + Y_{ij} \bar{Q}_{iL} \Phi Q_{jR} + Y'_{ij} \bar{Q}_{iL} \tilde{\Phi} Q_{jR} \\ & + \frac{1}{2} (f_L)_{ij} \ell_{iL}^T C i \sigma_2 \Delta_L \ell_{jL} + \frac{1}{2} (f_R)_{ij} \ell_{iR}^T C i \sigma_2 \Delta_R \ell_{jR} + \text{H.c.} \end{aligned} \quad (1)$$

where $\tilde{\Phi} = \tau_2 \Phi^* \tau_2$, C is the charge conjugation operator and the indices $i, j = 1, 2, 3$ correspond to the three generations of fermions. The Yukawa couplings involving the new fermions can be written as

$$\begin{aligned} \mathcal{L}_Y^{new} = & Y_\psi \bar{\psi} \tilde{H}_L N + Y_{\psi'} \bar{\psi}' \tilde{H}_R N + M \bar{\psi} \psi + M' \bar{\psi}' \psi' + f_\psi \sigma (\bar{\psi} \psi - \bar{\psi}' \psi') \\ & + Y_\phi \bar{\psi} \Phi \psi' + Y'_\phi \bar{\psi}' \tilde{\Phi} \psi' \end{aligned} \quad (2)$$

Particles	$SU(3)_c \times SU(2)_L \times SU(2)_R \times U(1)_{B-L} \times \mathbb{Z}_2$
Q_L	$(3, 2, 1, \frac{1}{3}, +)$
Q_R	$(3, 1, 2, \frac{1}{3}, +)$
ℓ_L	$(1, 2, 1, -1, +)$
ℓ_R	$(1, 1, 2, -1, +)$
ψ	$(1, 2, 1, -1, -)$
ψ'	$(1, 1, 2, -1, -)$
N	$(1, 1, 1, 0, -)$

TABLE I: Fermion content of the model

Particles	$SU(3)_c \times SU(2)_L \times SU(2)_R \times U(1)_{B-L} \times \mathbb{Z}_2$
Φ	$(1, 2, 2, 0, +)$
Δ_L	$(1, 3, 1, 2, +)$
Δ_R	$(1, 1, 3, 2, +)$
H_L	$(1, 2, 1, -1, +)$
H_R	$(1, 1, 2, -1, +)$
σ	$(1, 1, 1, 0, +)$

TABLE II: Scalar content of the model

The details of the scalar potential is given in appendix A. At a very high energy scale, the parity odd singlet σ can acquire a vev to break D-parity spontaneously while the neutral component of Δ_R acquires a non-zero vev at a later stage to break the gauge symmetry of the LRSM into that of the SM which then finally gets broken down to the $U(1)_{\text{em}}$ of electromagnetism by the vev of the neutral component of Higgs bidoublet Φ . Thus, the symmetry breaking chain is

$$\begin{aligned}
& SU(2)_L \times SU(2)_R \times U(1)_{B-L} \times D \xrightarrow{\langle \sigma \rangle} SU(2)_L \times SU(2)_R \times U(1)_{B-L} \xrightarrow{\langle \Delta_R \rangle} SU(2)_L \times U(1)_Y \\
& \xrightarrow{\langle \Phi \rangle} SU(2)_L \times U(1)_Y \xrightarrow{\langle \Phi \rangle} U(1)_{\text{em}}
\end{aligned}$$

Denoting the vev of the neutral components of the bidoublet as $k_{1,2}$ and that of triplet Δ_R

as v_R , the gauge boson masses after spontaneous symmetry breaking can be written as

$$M_{W_L}^2 = \frac{g^2}{4} k_1^2, \quad M_{W_R}^2 = \frac{g^2}{2} v_R^2, \\ M_{Z_L}^2 = \frac{g^2 k_1^2}{4 \cos^2 \theta_w} \left(1 - \frac{\cos^2 2\theta_w}{2 \cos^4 \theta_w} \frac{k_1^2}{v_R^2} \right), \quad M_{Z_R}^2 = \frac{g^2 v_R^2 \cos^2 \theta_w}{\cos 2\theta_w},$$

where θ_w is the Weinberg angle. The neutral components of the other scalar fields $H_{L,R}$ do not acquire any vev. However, the neutral component of the scalar triplet Δ_L can acquire a tiny but non-zero induced vev after the electroweak symmetry breaking as

$$v_L = \gamma \frac{M_{W_L}^2}{v_R}, \quad (3)$$

with $M_{W_L} \sim 80.4$ GeV being the weak boson mass and γ is a function of various couplings in the scalar potential. The bidoublet also gives rise to non-zero $W_L - W_R$ mixing parameterised by ξ as

$$\tan 2\xi = \frac{2k_1 k_2}{v_R^2 - v_L^2}, \quad (4)$$

which is constrained to be $\xi \leq 7.7 \times 10^{-4}$ [56, 57].

It should be noted that, our scenario can work even without the D-parity odd singlet scalar. In such a case, the parameters of the left and right sectors are equal until the $SU(2)_R \times U(1)_{B-L}$ symmetry breaking scale.

III. DECAY OF $Z_{L,R}$ INTO FIMP

The decay of $Z_{L,R}$ to the dark matter can occur at one loop level, the Feynman diagrams for which are shown in Fig. 1 :

The Lagrangian for the decay process is $-i\mathcal{A}\bar{N}\gamma^\mu\gamma_5 Z_{\mu L,R}N$ where the loop factor \mathcal{A} is given as:

$$\mathcal{A} = \frac{gY^*Y}{16\pi^2} \left[1 + \frac{m_{H_{L,R}}^2}{M_{Z_{L,R}}^2} \ln \left[\frac{2m_{H_{L,R}}^2 - M_{Z_{L,R}}^2 + \sqrt{M_{Z_{L,R}}^4 - 4m_{H_{L,R}}^2 M_{Z_{L,R}}^2}}{2m_{H_{L,R}}^2} \right]^2 \right], \quad (5)$$

if we take the limit $m_{H_{L,R}}^2 \ll M_{Z_{L,R}}^2$ and use the parametrisation $y = \frac{m_{H_{L,R}}^2}{M_{Z_{L,R}}^2}$, the loop factor can be written as

$$\mathcal{A} = \frac{gY^*Y}{16\pi^2} [1 + y \ln[y]^2 - \pi^2 y + 2i\pi \ln y + \mathcal{O}(y^2)].$$

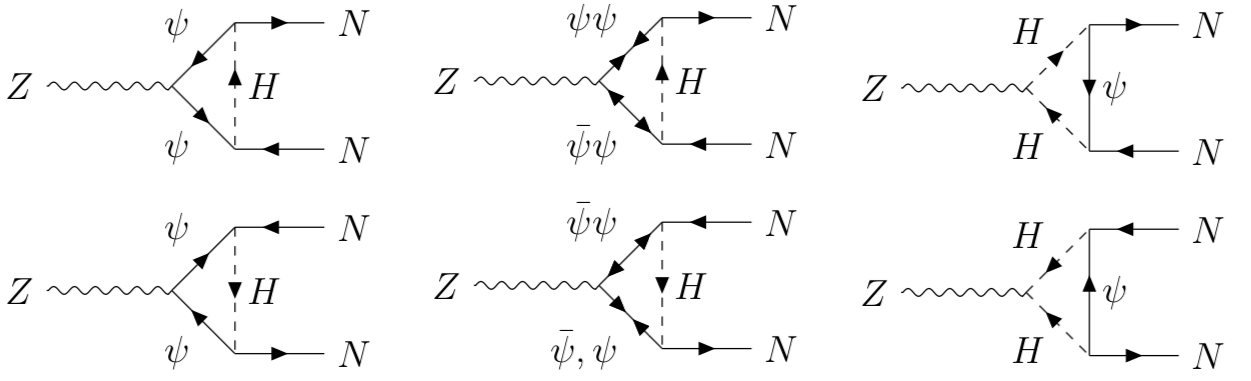


FIG. 1: The relevant decay diagrams for the $Z \rightarrow NN$ in two-spinor notation. Here for $Z = Z_L(Z_R)$, $f = \psi(\psi')$ and $H = H_L(H_R)$.

On the other hand, going to the other limit $m_{H_{L,R}}^2 \gg M_{Z_{L,R}}^2$ and parametrising $x = \frac{M_{Z_{L,R}}^2}{m_{H_{L,R}}^2}$ we can write

$$\mathcal{A} = \frac{gY^*Y}{16\pi^2} \left[-\frac{x}{12} + \mathcal{O}(x^{3/2}) \right] .$$

For further details about the loop diagram computation, please refer to Appendix B. In the above expression, all the masses of the particles inside the loop are taken to be same that is, $M_{\psi,\psi'} = M_{H_{L,R}} = m_\phi$. Also, the Yukawa couplings are denoted by a generalised notation Y which for Z_L as mother particle corresponds to Y_ψ and for Z_R as mother particle corresponds to $Y_{\psi'}$ shown in the Lagrangian in Eq. (2).

Since the particles inside loop have bare mass terms and hence can decouple, the form factor becomes very small for large mass for loop particles and in fact vanishes for $m_\phi \rightarrow \infty$. This behaviour can be seen from the plot of form factor as a function of $x = m_\phi^2/M_Z^2$ shown in Fig. 2. To show the dependence on loop particle masses alone, here we assume the Yukawa couplings to be unity. Suitable tuning of Yukawa couplings can help us to achieve the required vertex factor for freeze-in dark matter even if the loop particles are few times heavier than the decaying one.

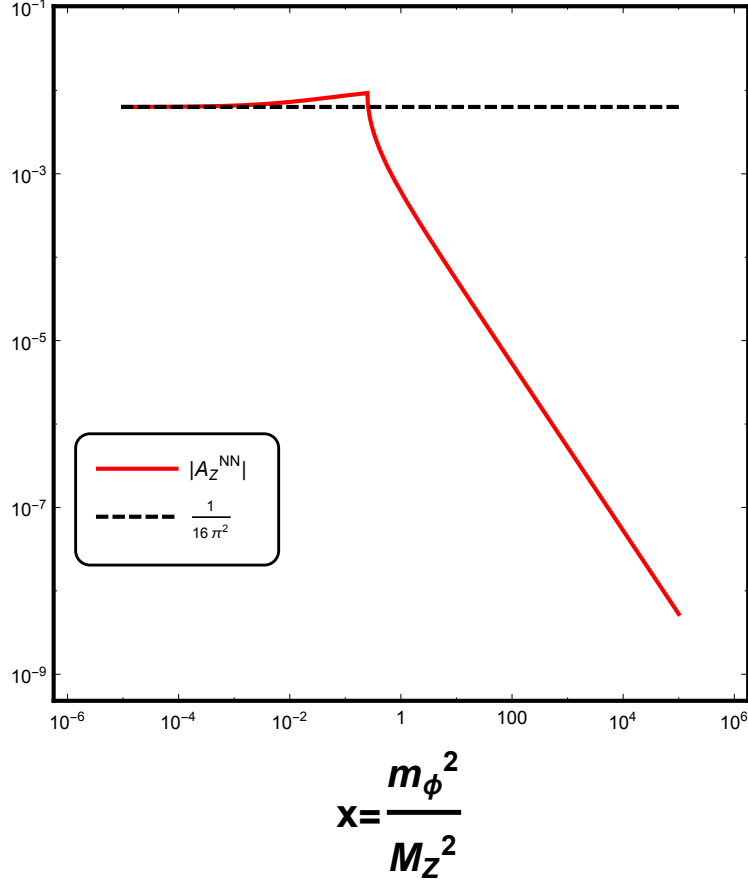


FIG. 2: Form factor for the one loop decay shown in figure 1.

IV. RELIC DENSITY CALCULATION

A. N as a natural FIMP candidate

In this model, as mentioned earlier, the fermion N is completely singlet under the left-right symmetry group $SU(2)_L \times SU(2)_R \times U(1)_{B-L}$ and it has an odd \mathbb{Z}_2 parity. However, being the lightest \mathbb{Z}_2 -odd particle, all the \mathbb{Z}_2 parity conserving decay modes of N are kinematically forbidden, making N absolutely stable over the cosmological time scale. Therefore, we consider N as a suitable dark matter candidate in this work. Apart from being the lightest \mathbb{Z}_2 -odd particle, N also fits into our desired FIMP scenario. This is due to the fact that, in the present model, all the portal interactions of N via $Z_{L,R}$ and Φ with the Standard Model particles are one loop suppressed. This naturally makes N very feebly interacting with the thermal bath and as a result N remains out of thermal equilibrium. Although N can thermalise with the plasma via t-channel scattering processes like $H_{L(R)} H_{L(R)} \rightarrow$

$\bar{N}N$, $\overline{\psi^{(l)}}\psi^{(l)} \rightarrow \bar{N}N$, $\psi^{(l)}H_{L(R)} \rightarrow NZ_{L(R)}$, $\psi^{(l)}H_{L(R)}^+ \rightarrow NW_{L(R)}^+$ etc, where the two N final states are suppressed by $Y_{\psi(\psi')}^4$ while the scattering processes with single N in the final state are proportional to $Y_{\psi(\psi')}^2$. Since, the Yukawa couplings are $Y_{\psi}Y_{\psi'} < 1$ in general, the dominant contribution arises from the scattering processes with single N in the final state. In the left panel of Fig. 3 we demonstrate the variation of ratio between the interaction rate $n_{\text{eq}}\langle\sigma v\rangle$ for the scattering process $\psi H_L \rightarrow NZ_L$ and the Hubble expansion rate \mathbf{H} with the temperature of the Universe T . In this plot, we have considered the masses of all the components of H_L and ψ to be equal and we have kept them fixed at 1 TeV. From this plot one can easily notice that the ratio $\frac{n_{\text{eq}}\langle\sigma v\rangle}{\mathbf{H}}$ is maximum when $T \sim 1$ TeV, same as the mass of incoming particles. After that, $\frac{n_{\text{eq}}\langle\sigma v\rangle}{\mathbf{H}}$ reduces with T as the equilibrium number density becomes exponentially suppressed for $T < 1$ TeV. We have plotted the variation of $\frac{n_{\text{eq}}\langle\sigma v\rangle}{\mathbf{H}}$ with respect to T for three different values of Yukawa coupling e.g. $Y_{\psi} = 10^{-4}$, 10^{-6} and 10^{-7} respectively. We have found that for $Y_{\psi} \geq 10^{-6}$, our DM candidate remains in thermal equilibrium with the plasma through the scattering $\psi^{(l)}H_{L(R)} \rightarrow NZ_{L(R)}$, as the interaction rate exceeds the Hubble expansion rate for the considered range of Temperature $10^2 \text{ GeV} \leq T \leq 10^4 \text{ GeV}$. However, as we reduce the Yukawa coupling further, the corresponding interaction rate also decreases ($\propto Y_{\psi}^2$) and we have found that for $Y_{\psi} \leq 10^{-7}$, N never thermalises with the bath particles. Therefore, the non-thermality condition $(n_{\text{eq}}\langle\sigma v\rangle/\mathbf{H} < 1)$ demands $Y_{\psi}, Y_{\psi'} \leq 10^{-7}$ ².

Nevertheless, one can still consider N as a non-thermal dark matter candidate without assuming such a low value for the Yukawa couplings. This is in fact, the prime motivation of this article, to realise FIMP dark matter without highly fine-tuned dimensionless couplings. In that case, we have to consider a scenario with low reheat temperature [58] of the Universe so that these particles $H_{L,R}, \psi, \psi'$ were not thermally produced in the early Universe, which actually prevents N to thermalise via scattering with H_L, H_R, ψ and ψ' . For example, the authors of [59] considered such heavy mediators having mass greater than the reheat temperature, but in a different dark matter scenario. Since the masses of these particles appear as bare mass terms in the Lagrangian and hence they do not depend upon the scale of symmetry breaking, we can push them high to any scale above the scale of reheating. Therefore, we do not really have to rely upon very specific inflationary models where low

² The similar bound on $Y_{\psi'}$ is coming from scattering involving ψ', H_R, N and Z_R .

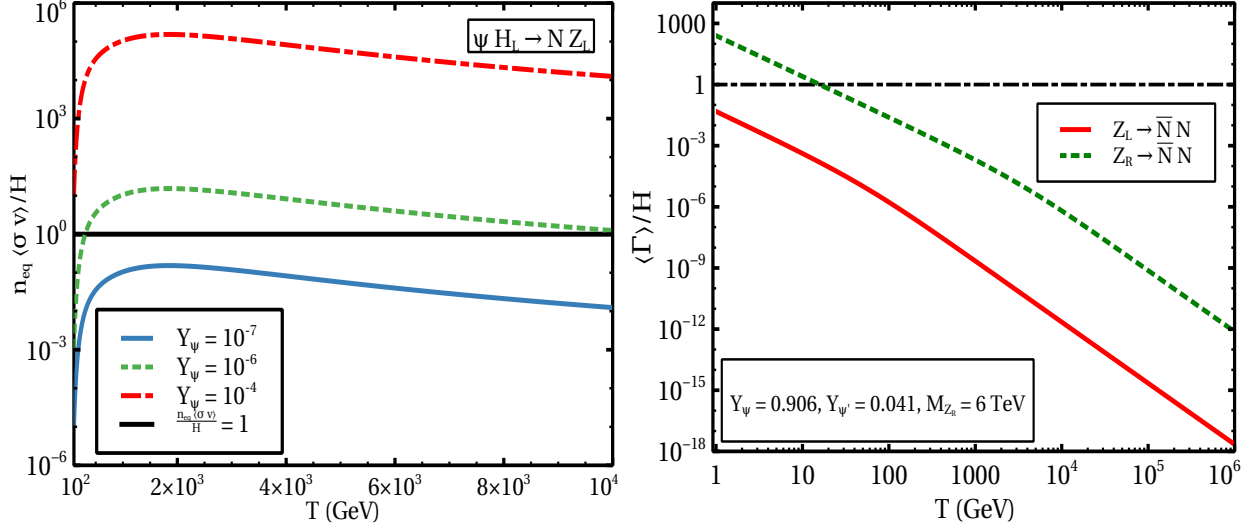


FIG. 3: Variation of ratio between interaction rate and Hubble expansion rate with temperature of the Universe. Left panel: plot for the scattering $\psi H_L \rightarrow N Z_L$. Right panel: plot for the decay modes $Z_{L,R} \rightarrow \bar{N}N$.

reheat temperature occurs. Such a setup leads to a situation where N can ‘talk’ to other particles in the thermal bath only through the one loop suppressed portals like Z_L , Z_R and Φ . In the right panel of Fig. 3, we plot the ratio of thermally averaged partial decay widths of $Z_{L,R}$ into two N ’s and H with T . Here, green dashed line represents the variation $\frac{\langle \Gamma \rangle}{H}$ with T for the right handed neutral gauge boson Z_R . In this plot, we have considered $M_{Z_R} = 6 \text{ TeV}$ and the corresponding Yukawa coupling $Y_{\psi'} = 0.041$ while the similar plot for the left handed neutral gauge boson Z_L has been drawn for $Y_\psi = 0.906$ and this is represented by the red solid line. From this figure, it is evident that for such moderately large Yukawa couplings (significantly larger compared to those required for scattering to be out of equilibrium) the decay rates of $Z_L \rightarrow \bar{N}N$, $Z_R \rightarrow \bar{N}N$ always lie below the Hubble expansion rate H , thus maintaining the non-thermality criteria of N . Although, for Z_R , the corresponding decay rate exceeds H when $T < 10 \text{ GeV}$, however at such low temperature the number density of Z_R with mass 6 TeV becomes exponentially suppressed and hence does have a very little impact on N . In fact, $\frac{\langle \Gamma \rangle}{H}$ for both Z_L and Z_R lie well below the expansion rate at $T \sim M_{Z_i}$ ($i = L, R$) where the maximum production of N from the decay of Z_i occurs. Therefore, N remains out of thermal equilibrium for moderately large values of Yukawa couplings ($\lesssim \mathcal{O}(1)$) and can be a candidate for FIMP accordingly. Note that the Yukawa couplings considered above are not fine tuned ones compared to those required in

generic FIMP models (IR Freeze-in scenarios).

B. The Boltzmann equation

The Boltzmann equation which governs the evaluation of comoving number density (ratio of number density to entropy density) of a FIMP is given by

$$\begin{aligned} \frac{dY_N}{dz} = & \frac{2M_{\text{Pl}}}{1.66M_{\text{sc}}^2} \frac{z\sqrt{g_\star(z)}}{g_s(z)} \left[\sum_{\chi=Z_L, Z_R, \Phi} \langle \Gamma_{\chi \rightarrow \bar{N}N} \rangle (Y_\chi^{\text{eq}} - Y_N) \right] \\ & + \frac{4\pi^2}{45} \frac{M_{\text{pl}}M_{\text{sc}}}{1.66} \frac{\sqrt{g_\star(z)}}{z^2} \left[\sum_{p=\text{SM fermions}} \langle \sigma v_{p\bar{p} \rightarrow \bar{N}N} \rangle \{ (Y_p^{\text{eq}})^2 - Y_N^2 \} \right]. \end{aligned} \quad (6)$$

where $z = \frac{M_{\text{sc}}}{T}$, is a dimensionless variable while M_{sc} is some arbitrary mass scale which we choose equal to the mass of Z_L and M_{Pl} is the Planck mass. Moreover, $g_s(z)$ is the number of effective degrees of freedom associated to the entropy density of the Universe and the quantity $g_\star(z)$ is defined as

$$\sqrt{g_\star(z)} = \frac{g_s(z)}{\sqrt{g_\rho(z)}} \left(1 - \frac{1}{3} \frac{d \ln g_s(z)}{d \ln z} \right). \quad (7)$$

Here, $g_\rho(z)$ denotes the effective number of degrees of freedom related to the energy density of the Universe at $z = \frac{M_{\text{sc}}}{T}$. The first term in the right hand side of the above Boltzmann equation (6) represents the production of our dark matter candidate N from the decays of Z_L , Z_R and bi-doublet Φ . The quantity Y_χ^{eq} is the equilibrium comoving number density of the species χ ($\chi = Z_L, Z_R, \Phi$) and in this work, except the dark matter candidate N , we consider Maxwell-Boltzmann distribution function for all the other particles which are in thermal equilibrium. As we have mentioned earlier, the production processes of N from the decays of Z_L , Z_R and Φ are one loop suppressed. The Feynman diagrams of these processes are shown in Fig. 1 and the corresponding one loop vertices are given in Eq. (5). Using the expressions of one loop vertices one can easily compute the thermally averaged decay width for the processes $Z_{L,R} \rightarrow \bar{N}N$ and expressions are given by,

$$\langle \Gamma_{Z_{L,R} \rightarrow \bar{N}N} \rangle = \Gamma_{Z_{L,R} \rightarrow \bar{N}N} \frac{K_1\left(\frac{M_{Z_{L,R}}}{T}\right)}{K_2\left(\frac{M_{Z_{L,R}}}{T}\right)}, \quad (8)$$

$$\Gamma_{Z_{L,R} \rightarrow \bar{N}N} = \frac{|\mathcal{A}_{Z_{L,R}}^{NN}|^2 M_{Z_{L,R}}}{24\pi} \left(1 - \frac{4M_N^2}{M_{Z_{L,R}}^2} \right)^{3/2}. \quad (9)$$

Where, $K_n \left(\frac{M_{Z_{L,R}}}{T} \right)$ is the n -th order modified Bessel function of second kind. The second term in the right hand side of the Boltzmann equation represents the contributions coming from the annihilations of SM particles to the production processes of N . Since N is a singlet under the left-right symmetry group, the interactions of N with the SM particles are possible only through the portal interactions by Z_L , Z_R and Φ beyond tree level. One could have a tree level coupling like $\bar{\ell}_L \tilde{H}_L N$ if the additional discrete symmetry \mathbb{Z}_2 was not in place. The other tree level couplings involving $H_{L,R}$, ψ , ψ' and N will not play a role in the production of N if these heavy incoming particles were not thermally produced in the early Universe due to their masses being heavier than the reheat temperature after inflation, as argued previously.

Hence, the contributions of such processes are sub-dominant compared to that from the decays of Z_L , Z_R , Φ as the couplings between our FIMP dark matter N and these mediator particles are one loop suppressed. In our calculations, we consider only the decay of the neutral gauge bosons Z_L , Z_R as they are more likely to be dominant due to the presence of gauge couplings in one of the vertices of the one loop diagram. For Φ decay diagram, one has more freedom in choosing another Yukawa coupling and hence that contribution can remain suppressed compared to the gauge boson ones.

Finally, the relic density of dark matter, which is defined as the ratio between dark matter mass density and critical density of the Universe, is obtained using the solution of Boltzmann equation ³ at the present epoch in the following equation [60]:

$$\Omega_{\text{DM}} h^2 = 2.755 \times 10^8 \left(\frac{M_N}{\text{GeV}} \right) Y_N(T_0), \quad (10)$$

where T_0 is the present temperature of the Universe $\sim \mathcal{O}(10^{-13})$ GeV.

C. Numerical results

In both panels of Fig. 4, we show the variation of comoving number density (Y_N) of N with the dimensionless variable $z = \frac{M_{Z_L}}{T}$. This plot has been generated for $M_{Z_R} = 6$ TeV, $M_N = 1$ MeV and three different values of Yukawa couplings Y_ψ and $Y_{\psi'}$ which reproduce the correct dark matter relic density. Moreover, in order to kinematically forbid the tree

³ In Appendix C, we have derived the analytical solution of the Boltzmann equation involving only decay terms in the R.H.S.

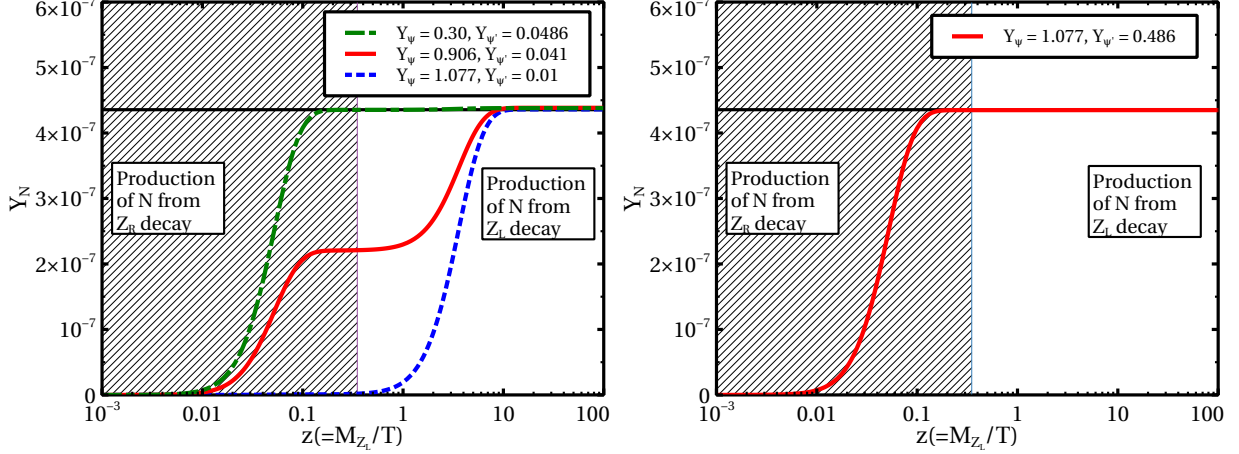


FIG. 4: Production of N in the early Universe when z changes from 0.001 to 100 for $M_L = M_R = 10^5$ GeV (left panel) and $M_L = M_R = 10^6$ GeV (right panel). For $M_L = M_R = 10^5$ GeV, N can be produced from both Z_L and Z_R depending upon the respective Yukawa couplings, however for $M_L = M_R = 10^6$ GeV, the decay of Z_R is the only dominant production mode of N if we restrict Y_ψ within the perturbative limit. Black solid line in both panels represents $Y_N = 4.356 \times 10^{-7}$, which reproduces $\Omega_N h^2 = 0.12$ for $M_N = 1$ MeV.

level decay of either H_L (H_R) or ψ (ψ') as well as to use the simple expressions for one loop decay widths in Eq. (5) we choose $M_{H_L} = M_\psi = M_L$ ($M_{H_R} = M_{\psi'} = M_R$). As mentioned earlier, we have also considered M_L , M_R , M , M' to be very large at least greater than the reheat temperature of the Universe after inflation, which can be sufficiently low (but higher than the mass scale of the decaying particles) in some cosmological scenarios like for example, [61, 62]. As a result, the production of N from the scatterings of these heavy particles is not efficient. The plot in the left panel is for $M_L = M_R = 10^5$ GeV. From this plot, it is seen that at first comoving number density of N increases as z increases from 0.01 to 0.1 (corresponding temperature decreases from $M_{Z_L}/0.01$ GeV to $M_{Z_L}/0.1$ GeV) and then for $0.1 \leq z \leq 0.35$, Y_N saturates to a particular value which depends upon the value of Yukawa coupling $Y_{\psi'}$ (e.g. green dashed-dotted line and red solid line). This initial rise in the comoving number density of N is due to its production from the heavy right handed neutral gauge boson Z_R . Since Z_R is in equilibrium with the thermal bath, most of the production of N from the decay of Z_R occurs for the temperature of the Universe $T \sim M_{Z_R}$. As the temperature drops below the mass of Z_R , the number density of Z_R starts

becoming exponentially suppressed (Boltzmann suppressed) and finally for $z \geq 0.1$ (or $T \leq 1$ TeV) there are practically not enough number of right handed neutral gauge boson left to produce N and thus the comoving number density Y_N saturates. Thereafter, again there is a sharp increase in the comoving number density of N between $z = 1.0$ to $z = 10$ (e.g. red solid line and blue dotted line). This increment of relic density is due to the substantial production of N from the decay of left handed neutral gauge boson Z_L (the usual Z boson in the SM), which depends on the other Yukawa coupling Y_ψ (see Eqs. (5) and (9)). Like the previous production regime of N from Z_R , in this case also the dominant production of N from Z_L decay occurs at around the temperature $T \sim M_{Z_L}$ ($z \sim 1$). Finally, when the temperature of the Universe drops well below the mass of Z_L , all the production modes of N cease and Y_N saturates to 4.356×10^{-7} , the value of Y_N which reproduces $\Omega_{\text{DM}} h^2 = 0.12$ for $M_N = 1$ MeV. Here, we have chosen three combinations of Yukawa couplings Y_ψ and $Y_{\psi'}$ which result in the correct relic density of dark matter. For $Y_\psi = 0.906$ and $Y_{\psi'} = 0.041$, we have a situation where there is an equal contribution of both Z_R and Z_L to Y_N and that is represented by the red solid line in Fig. 4. On the other hand by tuning both Y_ψ and $Y_{\psi'}$, one can have scenarios where the production of N is dominated by either Z_R or Z_L . These are described by green dashed-dotted line and blue dotted line respectively while the corresponding Yukawa couplings are $Y_\psi = 0.30$, $Y_{\psi'} = 0.0486$ and $Y_\psi = 1.077$, $Y_{\psi'} = 0.01$ respectively. Similarly, in the right panel we have shown the variation of Y_N with z for $M_L = M_R = 10^6$ GeV. However, unlike the plot in the left panel, here our DM candidate N is almost entirely produced from the decay of Z_R . This can be understood if we notice the expression of loop factor in the limit $M_{H_L} \gg M_{Z_L}$, where the loop factor is proportional to $x = M_{Z_L}^2/M_{H_L}^2$. Now, when we increase M_L ($= M_{H_L}$) from 10^5 GeV to 10^6 GeV, the corresponding loop factor for Z_L becomes suppressed by a factor of 10^2 and hence we need large Yukawa coupling Y_ψ to compensate this suppression. We have found that one cannot get any significant contribution from Z_L for $M_L = 10^6$ GeV as long as Y_ψ remains within the perturbative limit ($Y_\psi \leq \sqrt{4\pi}$).

The variation of Yukawa couplings Y_ψ and $Y_{\psi'}$ with M_L and M_R respectively has been shown in both panels of Fig. 5. In the left panel, we have shown the allowed parameter space in $Y_\psi - M_L$ plane which reproduces the observed dark matter relic density within 1σ limit. Now as we change Y_ψ and M_L , the loop factor for Z_L changes, which in turn modifies the contribution of Z_L to the relic density of N . The variation of the fractional contribution

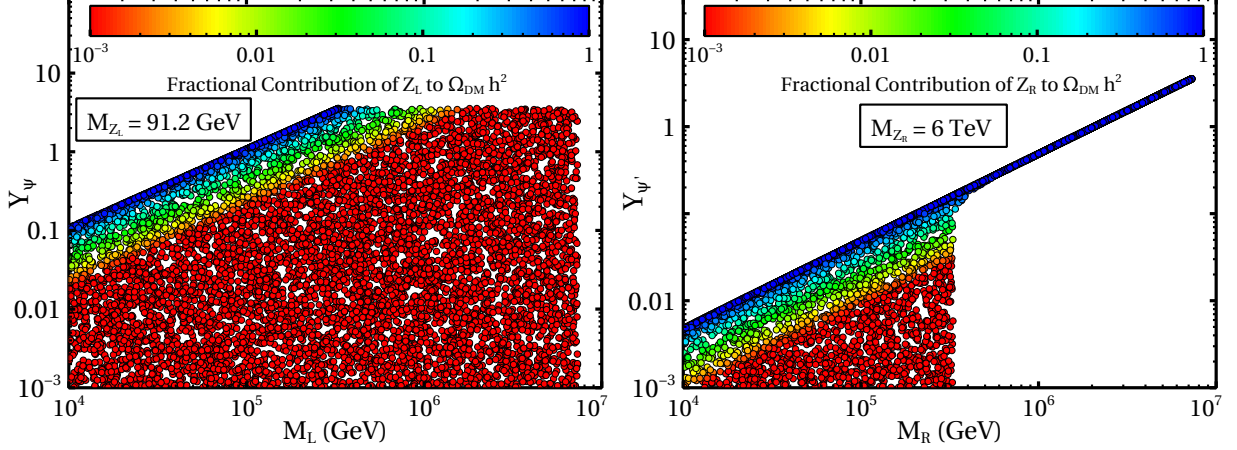


FIG. 5: Left panel: Variation of Y_ψ with M_L . Right panel: Variation of $Y_{\psi'}$ with M_R . Colour code in each panel represents the fractional contribution of the respective gauge boson to $\Omega_{\text{DM}} h^2$.

of Z_L ($\Omega_{\text{DM}}^{Z_L \rightarrow \bar{N}N} / \Omega_{\text{DM}}$) is shown by the colour code. The similar parameter space ($Y_{\psi'} - M_R$) for the right handed gauge boson Z_R is also shown in the right panel of Fig. 5. From the plot in the right panel it is seen that the fractional contribution of Z_R to $\Omega_{\text{DM}} h^2$ varies between 10^{-3} to 1 for $M_R \leq 4 \times 10^5$ GeV. Thereafter, Z_R becomes the dominant contributor for 4×10^5 GeV $< M_R < 8 \times 10^6$ GeV and beyond that ($M_R \geq 8 \times 10^6$ GeV) there is no allowed parameter space. This can be understood using the expression of loop factor for $Z_R(Z_L)$ in the limit $M_{Z_R}^2(M_{Z_L}^2) \ll M_R^2(M_L^2)$. In this limit, the loop factor for $Z_R(Z_L)$ is proportional to $\frac{M_R^2}{M_{Z_R}^2} \left(\frac{M_L^2}{M_{Z_L}^2} \right)$. Now, any increment in M_R and M_L decreases the corresponding loop factor and hence the contribution of the respective gauge boson to $\Omega_{\text{DM}} h^2$. This requires an enhancement in the Yukawa couplings. However, since $M_{Z_L} \ll M_{Z_R}$, the suppression of loop factor for Z_L is much more compared to that of Z_R for a particular value of M_L and M_R . Therefore, the contribution of Z_L becomes negligibly small for $M_L = M_R \gtrsim 5 \times 10^5$ GeV and $Y_\psi \leq \sqrt{4\pi}$ where the entire N production occurs from the decay of Z_R only. Similarly, if we keep on increasing M_R from 10^5 GeV to 10^7 GeV, we will encounter a situation for $M_R > 8 \times 10^6$ GeV when the loop factor of Z_R also becomes too small such that the Yukawa coupling $Y_{\psi'}$ within the perturbative limit is not enough to produce the right DM abundance.

In both panels of Fig. 6, we demonstrate the region in $Y_\psi - Y_{\psi'}$ plane which is allowed by the observed value of dark matter relic density at 68% C.L. ($0.1172 \leq \Omega_{\text{DM}} h^2 \leq 0.1226$). While generating these two plots we have scanned over the Yukawa couplings Y_ψ and $Y_{\psi'}$

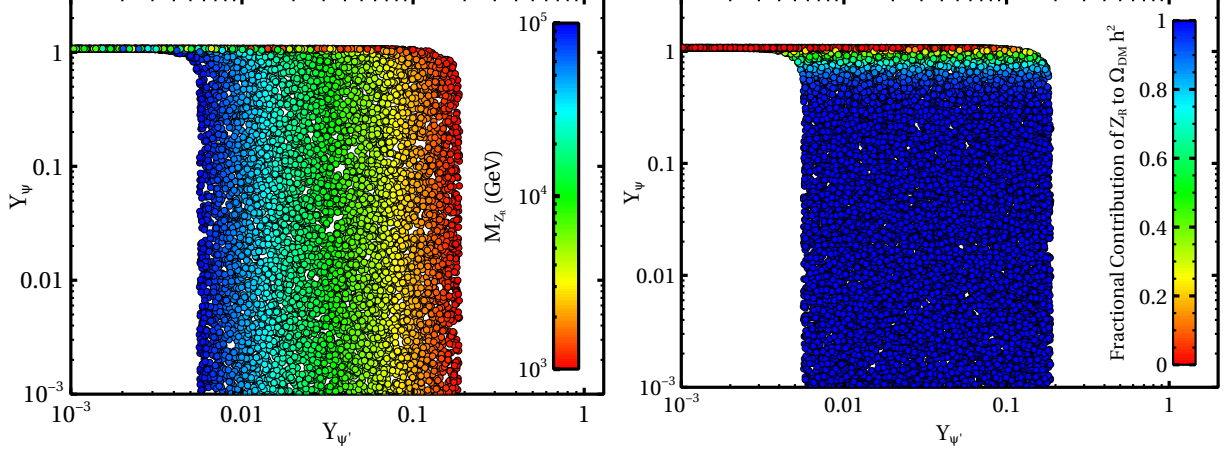


FIG. 6: Allowed region in $Y_\psi - Y_{\psi'}$ plane which reproduces correct dark matter relic density for $1 \text{ TeV} \leq M_{Z_R} \leq 100 \text{ TeV}$. We also shown the variation of M_{Z_R} (left panel) and the variation of the fractional contribution of Z_R to the relic density of N (right panel).

between $10^{-3} \leq Y_{\psi(\prime)} \leq \sqrt{4\pi}$ and the mass of Z_R in the range of 1 TeV to 100 TeV. The corresponding variation of M_{Z_R} in $Y_{\psi'} - Y_\psi$ plane has been shown by the colour code in the left panel. From this plot, one can notice that we need larger values of Yukawa coupling $Y_{\psi'}$ when M_{Z_R} decreases from 10^5 GeV to 10^3 GeV . This is because, the loop factor in the limit $M_{Z_R}^2 \ll M_R^2$ decreases with $x = M_{Z_R}^2/M_R^2$ and we need to enhance the Yukawa coupling $Y_{\psi'}$ appropriately to bring back the same contribution of Z_R to $\Omega_{\text{DM}} h^2$. In the right panel, we have drawn the same parameter space but in this case the colour code is used to demonstrate how the fractional contribution of Z_R to $\Omega_{\text{DM}} h^2$ changes with respect to the variation of the Yukawa couplings. The information about the fractional contribution of Z_L can also be obtained from this plot by subtracting the contribution of Z_R from unity. From this plot it is clearly seen that for $Y_{\psi'} > 5 \times 10^{-3}$ and $Y_\psi < 0.7$, the production of N is dominated by the Z_R decay and on the other hand, the relic density of N receives maximum contribution from Z_L when $Y_\psi \sim 1$. In the narrow intermediate region ($0.6 \leq Y_\psi \leq 1.0$ and $6 \times 10^{-3} \leq Y_{\psi'} \leq 0.2$), both Z_L and Z_R are contributing to the relic density of N and their contributions depend upon the specific values of Y_ψ and $Y_{\psi'}$. Moreover, we get a narrow horizontal line for $Y_\psi \sim 1$ and $Y_{\psi'} \lesssim 6 \times 10^{-3}$, where the entire production of N occurs from Z_L decay. The opposite situation where the entire N is produced from Z_R decay occurs for $Y_\psi < 0.6$ and $Y_{\psi'} > 6 \times 10^{-3}$. However, unlike to the Z_L dominated case, here we get a wide band and it due to the variation of mass of Z_R , which has been varied between 1 TeV to 100

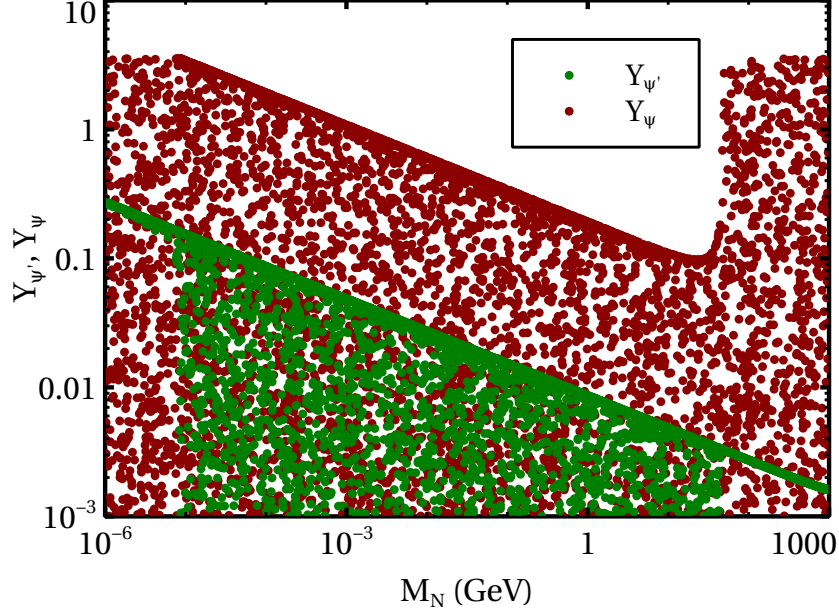


FIG. 7: The allowed values Y_{ψ} (dark red coloured contour) and $Y_{\psi'}$ (green coloured contour) from correct relic density criteria when M_N varies from 1 keV to 1 TeV.

TeV.

Finally, we have also shown the variation of Yukawa couplings Y_{ψ} and $Y_{\psi'}$ with the mass of our dark matter candidate N in Fig. 7. In this plot, we have varied M_N in the range of 1 keV to 1 TeV. The corresponding variation of $Y_{\psi'}$ (Y_{ψ}) to obtain the correct dark matter relic abundance is indicated by green (dark red) coloured contour. From this plot, one can notice that the allowed values of Yukawa couplings are decreasing with the increase of M_N . This can be understood from Eq. (10) which states that for a fixed value of $\Omega_{\text{DM}} h^2$ the product of $Y_N(t_0)$ and M_N is a constant. Since, our dark matter candidate is a FIMP, $Y_N(t_0)$ is proportional to the Yukawa couplings. Therefore, to remain within the observed relic density band, any increment in M_N must be accompanied by a decrement in $Y_N(t_0)$ and consequently in Y_{ψ} and $Y_{\psi'}$. In the right most corner of $M_N - Y_{\psi}$ plane, one can see that the entire range of Y_{ψ} is allowed for $M_N > M_{Z_L}/2$. This is due to the fact that in this mass range of N , the production from Z_L decay is kinematically forbidden and hence any variation in Y_{ψ} does not affect the relic density of N . On the other hand, as Z_L decay to a pair of N is not possible for $M_N > M_{Z_L}/2$, the decay Z_R is solely responsible for the entire production of N . Therefore, in this mass range of M_N , we get a very narrow allowed values of $Y_{\psi'}$. On the other hand, for low mass DM ($M_N \leq 5 \times 10^{-6}$ GeV) we also get a narrow

band for $Y_{\psi'}$ while all the values of other Yukawa coupling Y_{ψ} are allowed. This due to the fact that for the low dark matter mass, we need large $Y_N(t_0)$ to satisfy the relic density criterion as $\Omega_{DM}h^2$ is directly proportional to M_N and for Z_L to contribute significantly to $Y_N(t_0)$ we need Y_{ψ} beyond the perturbative regime. In other words in this low mass DM region Z_R again becomes the dominant contributor to DM relic abundance. Nevertheless, as the entire considered mass range of N is allowed for some combinations of Y_{ψ} and $Y_{\psi'}$, we have checked the nature of our dark matter candidate (hot/warm/cold) by computing its free streaming length following Ref. [63]. We find that N becomes a warm dark matter candidate for $M_N \leq 10$ keV, where its free streaming length goes above 0.01 Mpc. On the other hand, the cold dark matter scenario is viable for $M_N > 10$ keV, where the free streaming length of N always lies below 0.01 Mpc and decreases sharply with the increase of mass of N . The possibility of warm dark matter has several motivations, which can be found in the recent review [41].

V. CONCLUSION

We have proposed a UV complete framework to dynamically generate tiny couplings required for non-thermal dark matter scenarios whose relic abundance is generated through the freeze-in mechanism, within the framework called freeze-in massive particle. Based on gauge symmetric extensions of the Standard Model, we particularly consider the left-right symmetric model which have several other motivations related to the origin of parity violation, neutrino mass among others. Considering the dark matter candidate to be a gauge singlet fermion which has no tree level couplings with the Standard Model particles, we generate its couplings with the Standard Model particles at one loop, mediated by gauge bosons and Higgs. After showing such a dark matter candidate to remain out of thermal equilibrium in the early Universe for generic choices Yukawa couplings and masses of particles inside loops, we then calculate its relic abundance by considering both decay and scattering contributions in a way similar to a generic FIMP dark matter candidate. We find that the decay of neutral heavy gauge bosons to a pair of FIMP dark matter candidate is the most dominant production mechanism and can give rise to the correct relic abundance for Yukawa couplings as large as $\mathcal{O}(0.01)$ to $\mathcal{O}(1)$ while keeping the additional heavy neutral boson mass within experimental reach. Such Yukawa couplings lie in a range which less fine

tuned than the electron Yukawa coupling in the SM and far less fine tuned than the ones involved in generic FIMP models. On the other hand, a very wide range of dark matter masses is consistent with the relic abundance criteria and some portion of this allowed range can also give rise to warm dark matter scenarios that have several other motivations from small scale structure point of view. Since our UV complete setup has many other particles that lie in the experimentally accessible range, many associated particles can be probed at ongoing experiments, which we leave for future studies. We also note that such a setup can be realised in other gauge extensions of Standard Model as well which may be relatively simpler than the one presented here as a matter of choice.

Acknowledgments

DB acknowledges the support from IIT Guwahati start-up grant (reference number: xPHYSUGIITG01152xxDB001) and Associateship Programme of IUCAA, Pune. One of the authors AB acknowledges the financial support from SERB, Govt. of INDIA through NPDF fellowship with grant no. PDF/2017/000490. AB also gratefully acknowledges the cluster computing facility at HRI, Allahabad (<http://cluster.hri.res.in>).

Appendix A: Scalar Potential of the Model

The scalar potential for the minimal LRSM is

$$V(\Phi, \Delta_L, \Delta_R) = V_\mu + V_\Phi + V_\Delta + V_{\Phi\Delta} + V_{\Phi\Delta_L\Delta_R}, \quad (\text{A1})$$

where the bilinear terms in Higgs fields are

$$V_\mu = -\mu_1^2 \text{Tr}[\Phi^\dagger \Phi] - \mu_2^2 \text{Tr}[\Phi^\dagger \tilde{\Phi} + \tilde{\Phi}^\dagger \Phi] - \mu_3^2 \text{Tr}[\Delta_L^\dagger \Delta_L + \Delta_R^\dagger \Delta_R]. \quad (\text{A2})$$

The self-interaction terms of Φ are:

$$\begin{aligned} V_\Phi = & \lambda_1 [\text{Tr}[\Phi^\dagger \Phi]]^2 + \lambda_2 [\text{Tr}[\Phi^\dagger \tilde{\Phi}]]^2 + \lambda_2 [\text{Tr}[\tilde{\Phi}^\dagger \Phi]]^2 \\ & + \lambda_3 \text{Tr}[\Phi^\dagger \tilde{\Phi}] \text{Tr}[\tilde{\Phi}^\dagger \Phi] + \lambda_4 \text{Tr}[\Phi^\dagger \Phi] \text{Tr}[\Phi^\dagger \tilde{\Phi} + \tilde{\Phi}^\dagger \Phi]. \end{aligned} \quad (\text{A3})$$

and the $\Delta_{L,R}$ self- and cross-couplings are as follows:

$$\begin{aligned}
V_\Delta = & \rho_1 \left(\left[\text{Tr}[\Delta_L^\dagger \Delta_L] \right]^2 + \left[\text{Tr}[\Delta_R^\dagger \Delta_R] \right]^2 \right) + \rho_3 \text{Tr}[\Delta_L^\dagger \Delta_L] \text{Tr}[\Delta_R^\dagger \Delta_R] \\
& + \rho_2 \left(\text{Tr}[\Delta_L \Delta_L] \text{Tr}[\Delta_L^\dagger \Delta_L^\dagger] + \text{Tr}[\Delta_R \Delta_R] \text{Tr}[\Delta_R^\dagger \Delta_R^\dagger] \right) \\
& + \rho_4 \left(\text{Tr}[\Delta_L \Delta_L] \text{Tr}[\Delta_R^\dagger \Delta_R^\dagger] + \text{Tr}[\Delta_L^\dagger \Delta_L^\dagger] \text{Tr}[\Delta_R \Delta_R] \right). \tag{A4}
\end{aligned}$$

In addition, there are also $\Phi - \Delta_L$ and $\Phi - \Delta_R$ interactions present in the model,

$$\begin{aligned}
V_{\Phi\Delta} = & \alpha_1 \text{Tr}[\Phi^\dagger \Phi] \text{Tr}[\Delta_L^\dagger \Delta_L + \Delta_R^\dagger \Delta_R] + \alpha_3 \text{Tr}[\Phi \Phi^\dagger \Delta_L \Delta_L^\dagger + \Phi^\dagger \Phi \Delta_R \Delta_R^\dagger] \\
& + \left\{ \alpha_2 e^{i\delta_2} \text{Tr}[\Phi^\dagger \tilde{\Phi}] \text{Tr}[\Delta_L^\dagger \Delta_L] + \alpha_2 e^{i\delta_2} \text{Tr}[\tilde{\Phi}^\dagger \Phi] \text{Tr}[\Delta_R^\dagger \Delta_R] + \text{H.c.} \right\} \tag{A5}
\end{aligned}$$

with $\delta_2 = 0$ making CP conservation explicit, and the $\Phi - \Delta_L - \Delta_R$ couplings are

$$\begin{aligned}
V_{\Phi\Delta_L\Delta_R} = & \beta_1 \text{Tr}[\Phi^\dagger \Delta_L^\dagger \Phi \Delta_R + \Delta_R^\dagger \Phi^\dagger \Delta_L \Phi] + \beta_2 \text{Tr}[\Phi^\dagger \Delta_L^\dagger \tilde{\Phi} \Delta_R + \Delta_R^\dagger \tilde{\Phi}^\dagger \Delta_L \Phi] \\
& + \beta_3 \text{Tr}[\tilde{\Phi}^\dagger \Delta_L^\dagger \Phi \Delta_R + \Delta_R^\dagger \Phi^\dagger \Delta_L \tilde{\Phi}]. \tag{A6}
\end{aligned}$$

The scalar potential involving the newly introduced scalar fields beyond the minimal LRSM is

$$V_{\text{new}} = V_H + V_\sigma + V_{\Phi H} + V_{\Delta H}. \tag{A7}$$

The details of different terms on the right-hand side of the above equation can be written as follows,

$$\begin{aligned}
V_H = & \mu_H^2 (H_L^\dagger H_L + H_R^\dagger H_R) + \rho_5 \left(\left[H_L^\dagger H_L \right]^2 + \left[H_R^\dagger H_R \right]^2 \right) \\
& + \rho_6 \left[H_L^\dagger H_L \right] \left[H_R^\dagger H_R \right], \tag{A8}
\end{aligned}$$

$$\begin{aligned}
V_\sigma = & \frac{\mu_\sigma^2}{2} \sigma^2 + \rho_8 \sigma^4 + \mu_{\sigma\Delta} \sigma (\text{Tr}[\Delta_L^\dagger \Delta_L - \Delta_R^\dagger \Delta_R]) + \mu_{\sigma H} \sigma (H_L^\dagger H_L - H_R^\dagger H_R) \\
& + \rho_9 \sigma^2 \text{Tr}[\Phi^\dagger \Phi] + \rho_{10} \sigma^2 (\text{Tr}[\Delta_R^\dagger \Delta_R + \Delta_L^\dagger \Delta_L]) + \rho_{11} \sigma^2 (H_L^\dagger H_L + H_R^\dagger H_R), \tag{A9}
\end{aligned}$$

$$V_{\Phi H} = \mu_{14} H_L^\dagger \Phi H_R + f_{145} \text{Tr}[\Phi^\dagger \Phi] (H_L^\dagger H_L + H_R^\dagger H_R), \tag{A10}$$

$$\begin{aligned}
V_{\Delta H} = & (\mu_{15} H_L \Delta_L H_L + \mu_{16} H_R \Delta_R H_R + \text{H.c.}) + f_{145} (\text{Tr}[\Delta_L^\dagger \Delta_L] + \text{Tr}[\Delta_R^\dagger \Delta_R]) (H_L^\dagger H_L + H_R^\dagger H_R) \tag{A11}
\end{aligned}$$

Appendix B: Decay width calculation

In order to calculate the “Feeble” interaction which shows up radiatively, we would first like to briefly discuss the Lagrangian from which different vertices in the loop arise. The vertex involving gauge bosons and fermion/scalars will arise from the respective kinetic terms involving covariant derivatives. The covariant derivative for the gauge group of Left-Right model can be written as:

$$D_{L,R}^\mu = \left(\partial_\mu - ig_{L,R} \frac{\vec{\tau}}{2} \vec{W}_{L,R} - ig_{B-L} \frac{(\mathbf{B} - \mathbf{L})}{2} B_\mu \right) \quad (\text{B1})$$

Now, from the above covariant derivative the kinetic part of the Lagrangian for fermion doublets ψ , ψ' and scalar doublets H_L, H_R are as follows:

$$\mathcal{L}_{\text{kin}} \subset i\bar{\psi}\gamma_\mu D_L^\mu \psi + i\bar{\psi}'\gamma_\mu D_R^\mu \psi' + (D_{\mu R} H_R)^\dagger (D_R^\mu H_R) + (D_{\mu L} H_L)^\dagger (D_L^\mu H_L) \quad (\text{B2})$$

On the other hand, the scalar-fermion-fermion vertices in the loop diagrams arise from the corresponding Yukawa interactions shown in (2). Thus, the relevant interaction terms contributing to the one loop decay width of $Z_{L,R}$ into a pair of N 's are

$$\begin{aligned} \mathcal{L}_{\text{feeble}} \subset & \tilde{g}_L \bar{\psi} \gamma_\mu \psi Z_L^\mu + \tilde{g}_R \bar{\psi}' \gamma_\mu \psi' Z_R^\mu - i\tilde{g}_L (\partial_\mu H_L^\dagger H_L - H_L^\dagger \partial_\mu H_L) Z_L^\mu \\ & - i\tilde{g}_R (\partial_\mu H_R^\dagger H_R - H_R^\dagger \partial_\mu H_R) Z_R^\mu + Y_\psi \bar{\psi} \tilde{H}_L N + Y_{\psi'} \bar{\psi}' \tilde{H}_R N \end{aligned} \quad (\text{B3})$$

where $\tilde{g}_{L,R}$ are the respective gauge couplings in the physical basis of the neutral gauge bosons. The decay of $Z_{L,R}$ to pair of FIMP's (N 's) from the above Lagrangian are shown in Fig.1 and we closely follow the two-spinor technique [64] in order to calculate the loop factors and the aforementioned figure is also shown using the same notations.

The Lagrangian for the above decay process is $-i\mathcal{A}\bar{N}\gamma^\mu\gamma^5 Z_{\mu L,R}N$ where the loop factor \mathcal{A} is given as:

$$\mathcal{A} = \frac{i\tilde{g}Y^2}{16\pi^2} \left[1 + \frac{m_{H_{L,R}}^2}{M_{Z_{L,R}}^2} \ln \left[\frac{2m_{H_{L,R}}^2 - M_{Z_{L,R}}^2 + \sqrt{M_{Z_{L,R}}^4 - 4m_{H_{L,R}}^2 M_{Z_{L,R}}^2}}{2m_{H_{L,R}}^2} \right]^2 \right]. \quad (\text{B4})$$

If we take the limit $m_{H_{L,R}}^2 \ll M_{Z_{L,R}}^2$ and use the parametrisation $y = \frac{m_{H_{L,R}}^2}{M_{Z_{L,R}}^2}$, then the loop factor is

$$\mathcal{A} = \frac{i\tilde{g}Y^2}{16\pi^2} [1 + y \ln[y]^2 - \pi^2 y + 2i\pi \ln y + \mathcal{O}(y^2)].$$

On the other hand, going to the other limit $m_{H_{L,R}}^2 \gg M_{Z_{L,R}}^2$ and parametrising $x = \frac{M_{Z_{L,R}}^2}{m_{H_{L,R}}^2}$ we can write the loop factor as

$$\mathcal{A} = \frac{i\tilde{g}Y^2}{16\pi^2} \left[-\frac{x}{12} + \mathcal{O}(x^{3/2}) \right].$$

It should be noted that, we have explicitly written the interaction term of gauge bosons with a pair of N 's as axial vector couplings. This is due to the Majorana nature of fermion N . Let us take a detour in showing why Majorana particle cannot have vector like interaction. Let us start with the following general interaction for Majorana particle $N = N^c$ (where N^c is charge conjugated field of N)

$$\begin{aligned} \frac{1}{2}\bar{N}(g_V\gamma^\mu + g_A\gamma^\mu\gamma^5)N &= \frac{1}{2}\bar{N}^c(g_V\gamma^\mu + g_A\gamma^\mu\gamma^5)N^c \\ &= \frac{g_V}{2}\overline{C\bar{N}^T}\gamma^\mu C\bar{N}^T + \frac{g_A}{2}\overline{C\bar{N}^T}\gamma^\mu\gamma^5 C\bar{N}^T \\ &= \frac{g_V}{2}(C\bar{N}^T)^\dagger\gamma^0\gamma^\mu C\bar{N}^T + \frac{g_A}{2}(C\bar{N}^T)^\dagger\gamma^0\gamma^\mu CC^{-1}\gamma^5 C\bar{N}^T \\ &= \frac{g_V}{2}\bar{N}^*C^{-1}\gamma^0\gamma^\mu C\bar{N}^T + \frac{g_A}{2}\bar{N}^*C^{-1}\gamma^0\gamma^\mu C\gamma^{5T}\bar{N}^T \\ &= \frac{g_V}{2}N^T\gamma^{0*}C^{-1}\gamma^0 CC^{-1}\gamma^\mu C\bar{N}^T + \frac{g_A}{2}N^T\gamma^{0*}C^{-1}\gamma^0 CC^{-1}\gamma^\mu C\gamma^{5T}\bar{N}^T \\ &= -\frac{g_V}{2}N^T\gamma^{0*}\gamma^{0T}C^{-1}\gamma^\mu C\bar{N}^T - \frac{g_A}{2}N^T\gamma^{0*}\gamma^{0T}C^{-1}\gamma^\mu C\gamma^{5T}\bar{N}^T \\ &= -\frac{g_V}{2}N^TC^{-1}\gamma^\mu C\bar{N}^T - \frac{g_A}{2}N^TC^{-1}\gamma^\mu C\gamma^{5T}\bar{N}^T \\ &= +\frac{g_V}{2}N^T\gamma^{\mu T}\bar{N}^T + \frac{g_A}{2}N^T\gamma^{\mu T}\gamma^{5T}\bar{N}^T \\ &= -\frac{g_V}{2}\bar{N}\gamma^\mu N + \frac{g_A}{2}\bar{N}\gamma^\mu\gamma^5 N \\ g_V\bar{N}\gamma^\mu N &= 0 \end{aligned} \tag{B5}$$

which justifies the use of axial vector like couplings of N 's with gauge bosons.

Appendix C: Analytical solution of Boltzmann equation

In this section, we present analytical solution of the Boltzmann equation considering dark matter production through decays of heavy particles only. Once we derive the analytical expression of comoving number density (Y_N) for decays then the same procedure can be followed to find Y_N due to scattering processes. In terms of Y_N the Boltzmann equation for

N , due to its production from the decays of Z_L , Z_R and Φ , is given by,

$$\frac{dY_N}{dz} = \frac{2M_{\text{Pl}}}{1.66M_{sc}^2} \frac{z\sqrt{g_*(z)}}{g_s(z)} \left[\sum_{\chi=Z_L, Z_R, \Phi} \langle \Gamma_{\chi \rightarrow \bar{N}N} \rangle (Y_\chi^{\text{eq}} - Y_N) \right], \quad (\text{C1})$$

where, M_{sc} is some arbitrary mass scale which we consider equal to M_{Z_L} . Now, since N is a dark matter candidate of non-thermal origin, we can neglect Y_N in the R.H.S. of the above equation due to its smallness compared to Y_χ ($\chi = Z_L, Z_R$ and Φ) of mother particles which are in thermal equilibrium and obey the Maxwell-Boltzmann distribution. Hence Y_χ^{eq} can be expressed as

$$Y_\chi^{\text{eq}}(z) = \frac{45 g_\chi}{4\pi^4} \frac{r_\chi^2 z^2 K_2(r_\chi z)}{g_s(z)}, \quad (\text{C2})$$

where, $r_\chi = \frac{M_\chi}{M_{sc}}$ is the ratio between M_χ and M_{sc} . Moreover, $g_s(z)$ being the total degrees of freedom of all relativistic species contributing to the entropy density of the Universe at $z = M_{sc}/T$. The expression of $\langle \Gamma_{\chi \rightarrow \bar{N}N} \rangle$ is given by

$$\langle \Gamma_{\chi \rightarrow \bar{N}N} \rangle = \Gamma_{\chi \rightarrow \bar{N}N} \frac{K_1(r_\chi z)}{K_2(r_\chi z)}. \quad (\text{C3})$$

Substituting Eqs. (C2) and (C3) in Eq. (C1) we get,

$$\frac{dY_N}{dz} = \frac{2M_{\text{Pl}}}{1.66M_{sc}^2} \frac{45}{4\pi^4} \frac{\sqrt{g_*(z)}}{g_s(z)^2} \sum_{\chi=Z_L, Z_R, \Phi} g_\chi r_\chi^2 \Gamma_{\chi \rightarrow \bar{N}N} K_1(r_\chi z) z^3. \quad (\text{C4})$$

Now, $\frac{\sqrt{g_*(z)}}{g_s(z)^2} \simeq \frac{1}{\sqrt{g_\rho(z)} g_s(z)}$ where $g_\rho(z)$ is the total relativistic degrees of freedom contributing to the energy density of the Universe at $z = M_{sc}/T$. Here, we have neglected the a term proportional to $\frac{d \ln g_s(z)}{d \ln z}$ (see Eq. (7)), which becomes important only around the QCD phase transition temperature ($T \sim \mathcal{O}(100)$ MeV), where $g_s(z)$ changes drastically with z [7]. Therefore, the Eq. (C4) simplifies to

$$\frac{dY_N}{dz} = \frac{2M_{\text{Pl}}}{1.66} \frac{45}{4\pi^4} \frac{1}{\sqrt{g_\rho(z)} g_s(z)} \sum_{\chi=Z_L, Z_R, \Phi} \frac{g_\chi r_\chi^4}{M_\chi^2} \Gamma_{\chi \rightarrow \bar{N}N} K_1(r_\chi z) z^3, \quad (\text{C5})$$

and therefore

$$Y_N = \frac{2M_{\text{Pl}}}{1.66} \frac{45}{4\pi^4} \sum_{\chi=Z_L, Z_R, \Phi} \frac{g_\chi r_\chi^4}{M_\chi^2} \Gamma_{\chi \rightarrow \bar{N}N} \int_{z_{\min}}^{z_{\max}} \frac{K_1(r_\chi z) z^3}{\sqrt{g_\rho(z)} g_s(z)} dz. \quad (\text{C6})$$

$z_{\{min, max\}}$ correspond to initial and final temperatures respectively. One can further simplify the above equation to

$$Y_N \simeq \frac{2 M_{\text{Pl}}}{1.66} \frac{45}{4\pi^4} \sum_{\chi=Z_L, Z_R, \Phi} \frac{g_\chi}{M_\chi^2 \sqrt{g_\rho} g_s} \Gamma_{\chi \rightarrow \bar{N} N} \int_{x_{min}}^{x_{max}} K_1(x) x^3 dx, \quad (\text{C7})$$

where g_ρ, g_s are evaluated at $T = M_\chi$ and $x = r_\chi z$. The above integral is maximum around $x \sim 1$ (or $T \sim M_\chi$), where we assume g_ρ, g_s remain nearly constant. This is a reasonable assumption as long as T is far away from the QCD phase transition temperature. Now, considering x_{min} and x_{max} equal to 0 and ∞ , the expression Y_N becomes

$$Y_N \simeq 2 \frac{135 M_{\text{Pl}}}{8\pi^3 1.66} \sum_{\chi=Z_L, Z_R, \Phi} \frac{1}{\sqrt{g_\rho} g_s} \left(\frac{g_\chi \Gamma_{\chi \rightarrow \bar{N} N}}{M_\chi^2} \right). \quad (\text{C8})$$

The above expression of comoving number density for N is similar to the expression given in [15], except the factor 2, which is appearing due to the production to two N s in the final state from a single decay of χ .

-
- [1] F. Zwicky, *Helv. Phys. Acta* **6**, 110 (1933), [*Gen. Rel. Grav.*41,207(2009)].
 - [2] V. C. Rubin and W. K. Ford, Jr., *Astrophys. J.* **159**, 379 (1970).
 - [3] D. Clowe, M. Bradac, A. H. Gonzalez, M. Markevitch, S. W. Randall, C. Jones, and D. Zaritsky, *Astrophys. J.* **648**, L109 (2006), astro-ph/0608407.
 - [4] G. Hinshaw et al. (WMAP), *Astrophys. J. Suppl.* **208**, 19 (2013), 1212.5226.
 - [5] P. A. R. Ade et al. (Planck), *Astron. Astrophys.* **594**, A13 (2016), 1502.01589.
 - [6] M. Srednicki, R. Watkins, and K. A. Olive, *Nucl. Phys.* **B310**, 693 (1988) .
 - [7] P. Gondolo and G. Gelmini, *Nucl. Phys.* **B360**, 145 (1991).
 - [8] G. Jungman, M. Kamionkowski, and K. Griest, *Phys. Rept.* **267**, 195 (1996), hep-ph/9506380.
 - [9] G. Bertone, D. Hooper, and J. Silk, *Phys. Rept.* **405**, 279 (2005), hep-ph/0404175.
 - [10] G. Arcadi, M. Dutra, P. Ghosh, M. Lindner, Y. Mambrini, M. Pierre, S. Profumo, and F. S. Queiroz, *Eur. Phys. J.* **C78**, 203 (2018), 1703.07364.
 - [11] A. Tan et al. (PandaX-II), *Phys. Rev. Lett.* **117**, 121303 (2016), 1607.07400.
 - [12] E. Aprile et al. (XENON), *Phys. Rev. Lett.* **119**, 181301 (2017), 1705.06655.
 - [13] D. S. Akerib et al. (LUX), *Phys. Rev. Lett.* **118**, 021303 (2017), 1608.07648.
 - [14] F. Kahlhoefer, *Int. J. Mod. Phys.* **A32**, 1730006 (2017), 1702.02430.

- [15] L. J. Hall, K. Jedamzik, J. March-Russell, and S. M. West, JHEP **03**, 080 (2010), 0911.1120.
- [16] A. Biswas and A. Gupta, JCAP **1609**, 044 (2016), [Addendum: JCAP1705,no.05,A01(2017)], 1607.01469.
- [17] A. Biswas, S. Choubey, and S. Khan, Eur. Phys. J. **C77**, 875 (2017), 1704.00819.
- [18] N. Bernal, M. Heikinheimo, T. Tenkanen, K. Tuominen, and V. Vaskonen, Int. J. Mod. Phys. **A32**, 1730023 (2017), 1706.07442.
- [19] G. Arcadi and L. Covi, JCAP **1308**, 005 (2013), 1305.6587.
- [20] C. E. Yaguna, JHEP **08**, 060 (2011), 1105.1654.
- [21] M. Blennow, E. Fernandez-Martinez, and B. Zaldivar, JCAP **1401**, 003 (2014), 1309.7348.
- [22] A. Merle and M. Totzauer, JCAP **1506**, 011 (2015), 1502.01011.
- [23] B. Shakya, Mod. Phys. Lett. **A31**, 1630005 (2016), 1512.02751.
- [24] J. König, A. Merle, and M. Totzauer, JCAP **1611**, 038 (2016), 1609.01289.
- [25] A. Biswas and A. Gupta, JCAP **1703**, 033 (2017), [Addendum: JCAP1705,no.05,A02(2017)], 1612.02793.
- [26] A. Biswas, S. Choubey, and S. Khan, JHEP **02**, 123 (2017), 1612.03067.
- [27] F. Elahi, C. Kolda, and J. Unwin, JHEP **03**, 048 (2015), 1410.6157.
- [28] J. McDonald, JCAP **1608**, 035 (2016), 1512.06422.
- [29] D. E. Kaplan and R. Rattazzi, Phys. Rev. **D93**, 085007 (2016), 1511.01827.
- [30] G. F. Giudice and M. McCullough, JHEP **02**, 036 (2017), 1610.07962.
- [31] J. Kim and J. McDonald (2017), 1709.04105.
- [32] J. Kim and J. McDonald (2018), 1804.02661.
- [33] J. C. Pati and A. Salam, Phys. Rev. **D10**, 275 (1974), [Erratum: Phys. Rev.D11,703(1975)].
- [34] R. N. Mohapatra and J. C. Pati, Phys. Rev. **D11**, 2558 (1975).
- [35] G. Senjanovic and R. N. Mohapatra, Phys. Rev. **D12**, 1502 (1975).
- [36] R. N. Mohapatra and R. E. Marshak, Phys. Rev. Lett. **44**, 1316 (1980), [Erratum: Phys. Rev. Lett.44,1643(1980)].
- [37] N. G. Deshpande, J. F. Gunion, B. Kayser, and F. I. Olness, Phys. Rev. **D44**, 837 (1991).
- [38] M. Nemevsek, G. Senjanovic, and Y. Zhang, JCAP **1207**, 006 (2012), 1205.0844.
- [39] F. Bezrukov, H. Hettmansperger, and M. Lindner, Phys. Rev. **D81**, 085032 (2010), 0912.4415.
- [40] D. Borah and A. Dasgupta (2017), 1710.06170.
- [41] M. Drewes et al., JCAP **1701**, 025 (2017), 1602.04816.

- [42] M. Cirelli, N. Fornengo, and A. Strumia, Nucl. Phys. **B753**, 178 (2006), hep-ph/0512090.
- [43] C. Garcia-Cely, A. Ibarra, A. S. Lamperstorfer, and M. H. G. Tytgat, JCAP **1510**, 058 (2015), 1507.05536.
- [44] M. Cirelli, T. Hambye, P. Panci, F. Sala, and M. Taoso, JCAP **1510**, 026 (2015), 1507.05519.
- [45] J. Heeck and S. Patra, Phys. Rev. Lett. **115**, 121804 (2015), 1507.01584.
- [46] C. Garcia-Cely and J. Heeck (2015), [JCAP1603,021(2016)], 1512.03332.
- [47] D. Borah and A. Dasgupta, JHEP **01**, 072 (2017), 1609.04236.
- [48] D. Borah, A. Dasgupta, and S. Patra (2016), 1604.01929.
- [49] A. Berlin, P. J. Fox, D. Hooper, and G. Mohlabeng, JCAP **1606**, 016 (2016), 1604.06100.
- [50] D. Borah, Phys. Rev. **D94**, 075024 (2016), 1607.00244.
- [51] D. Borah and A. Dasgupta, JCAP **1706**, 003 (2017), 1702.02877.
- [52] D. Borah, A. Dasgupta, U. K. Dey, S. Patra, and G. Tomar (2017), 1704.04138.
- [53] P. S. B. Dev, D. Kazanas, R. N. Mohapatra, V. L. Teplitz, and Y. Zhang, JCAP **1608**, 034 (2016), 1606.04517.
- [54] P. S. Bhupal Dev, R. N. Mohapatra, and Y. Zhang, JHEP **11**, 077 (2016), 1608.06266.
- [55] P. S. B. Dev, R. N. Mohapatra, and Y. Zhang (2016), 1610.05738.
- [56] G. Aad et al. (ATLAS), Eur. Phys. J. **C72**, 2056 (2012), 1203.5420.
- [57] S. Chatrchyan et al. (CMS), Phys. Rev. Lett. **109**, 261802 (2012), 1210.2402.
- [58] P. F. de Salas, M. Lattanzi, G. Mangano, G. Miele, S. Pastor, and O. Pisanti, Phys. Rev. **D92**, 123534 (2015), 1511.00672.
- [59] Y. Mambrini, K. A. Olive, J. Quevillon, and B. Zaldivar, Phys. Rev. Lett. **110**, 241306 (2013), 1302.4438.
- [60] J. Edsjo and P. Gondolo, Phys. Rev. **D56**, 1879 (1997), hep-ph/9704361.
- [61] T. Moroi, H. Murayama, and M. Yamaguchi, Phys. Lett. **B303**, 289 (1993).
- [62] A. de Gouvea, T. Moroi, and H. Murayama, Phys. Rev. **D56**, 1281 (1997), hep-ph/9701244.
- [63] A. Merle, V. Niro, and D. Schmidt, JCAP **1403**, 028 (2014), 1306.3996.
- [64] H. K. Dreiner, H. E. Haber, and S. P. Martin, Phys. Rept. **494**, 1 (2010), 0812.1594.